QIAU

Journal of Structural Engineering and Geotechnics

12(2), 25-43, Summer & Autumn 2022

JSEG

A Parametric Study of Interactions Between Liquefaction Sand Lenses and Shallow Tunnels Under Earthquake Loads

Mohammad Shabani Soltan Moradi [a], Mohammad Azadi [a,*], homayoun jahanian[a]

[a]*Department of Civil Engineering, Qazvin Branch, Islamic Azad University, Qazvin, Iran*

Received 12 September 2022, Accepted 22 September 2022

Abstract

If the saturated sand lenses are placed around the tunnels under the force of the earthquake, liquefaction will occur in them. This will cause settlement of the ground surface and changes in forces and anchors on the tunnel lining. For this purpose, it is important to evaluate the change of different parameters of the sand lens and the change of the thickness of the tunnel lining in the part of the sand lens and the changes in the diameter and depth of the tunnel as well as the location of the sand lens considering the tunnel inside it. Therefore, this article investigates the mentioned changes in shallow tunnels in the location of sand lens in flowing soils surrounded by clay. In this article, FLAC 3D software is used to determine changes in pore water pressure and effective stress reduction after sand lens liquefaction. Based on the obtained results, if the sand lenses are placed at a depth of less than 10 meters, they increase the land surface subsidence by 36% compared to the reference model B, with an increase of 2 meters in the depth of the sand lens compared to the reference model B, the value of the maximum bending anchor and axial force on the tunnel lining increases by 35.7% and 14.4%, respectively, in the sand lens part. The findings of the present study can be very useful in the decision-making process of tunnels that are dug inside flowing sand lenses.

Keywords: liquefaction, tunnel, sand lens, pore water pressure, effective stress.

1-Introduction

In the event of an earthquake, it is sometimes observed that seemingly un-liquefied soil has undergone large non-uniform deformations. This phenomenon is mostly observed near rivers or shores. Geological evaluations show that while the soil has suitable resistance parameters, weak sand lenses within the soil can become liquefied in the case of an earthquake. Although these lenses have a high static load resistance, if seismic loads are exerted on them, they can quickly lose their resistance and become a viscous liquid. This has severe implications for underground structures such as tunnels.

The earthquakes in Alaska (1964), Guam (1993) and Seattle (2001) are examples of this type of soil liquefaction and were accompanied with massive structural damages. Tunnels built in these types of soils can be affected by soil liquefaction which causes changes in the shape of the tunnel lining, ground surface settlement and increased pore water pressure[1].

Many studies have been conducted on sand lens liquefaction. Vallejo et al. investigated the effects of sand lens liquefaction in clay deposits and calculated the failure angle caused by soil liquefaction. Their results showed that sand lens liquefaction had caused a crack with an angle of 70.5° located at one corner of the lens inside the clay sediment along with an additional shear failure at another corner[2]. As can be seen in Figure 1, sand lens liquefaction can cause ground surface settlement which will deform any structure built at this area.

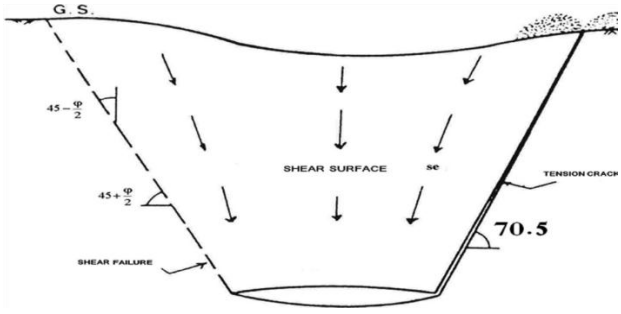

Fig.1. The effects of sand lens liquefaction on the surrounding soil [2].

*Corresponding Author: Email Address: Azadi.mhmm@gmail.com

Shokri et al. used elastic behavior models to analyze this phenomenon[3]. Beheshti et al. used the NISA software solution for their analysis and concluded that the elastoplastic behavior model of soil is a good approximation of their results[4]. It can thus be concluded that the Mohr–Coulomb model can be used in the present study. Mirhoseini et al. studied sand lens liquefaction locations around low depth tunnels while exerting seismic loads[5]. Azadi et al. investigated the relationship between ground surface settlement and the width of the sand lens in low depth tunnels[6].

Other studies have also been conducted regarding soil liquefaction around tunnels[7, 8]. Some studies have used shaking tables in order to determine the various forces and moments exerted on tunnel linings as a result of soil liquefaction[9]. Gang Zheng et al. used the SVM model along with Artificial Neural Networks (ANN) in order to evaluate tunnels at risk of soil liquefaction[10].

Qing Liao et al.[11],Using artificial neural network and multi-objective optimization, Liao et al., investigated various parameters of tunnels that are exposed to liquefaction and announced that two or more opposing objectives can be simultaneously optimized by multi-objective optimization. Nokande et al.[12], conducted several experiments using the shaking table to reduce the uplift of shallow tunnels during liquefaction and stated that helical piles can effectively limit the possibility of rapid tunnel uplift. Chian et al. studied the relationship between soil displacement, soil unit weight and tunnel diameter[13]. Azadi et al. analyzed soil stress around tunnels built in areas susceptible to liquefaction and included pore water pressure and an analysis of the effective stresses at both the upper and lower portions of the tunnel[14].

Studies conducted by other researchers so far have mostly focused on the aforementioned parameters in soils susceptible to liquefaction. Few studies can be found that have looked at these parameters inside the sand lens itself. This includes the evaluation of tunnel lining thickness inside the sand lens, changing the angle of friction within a liquefaction sand lens that resides within a non-liquefiable medium (clay soil) while various earthquakes are being exerted onto them, as well as evaluating the depth of the liquefaction sand lens that the tunnel is residing in. Additionally, the present study evaluated different tunnel diameters at various depths within the liquefaction sand lens. The issues mentioned above distinguish the present study from previous research conducted in this regard. Thus, considering the importance of this subject, the presents study was conducted with the aim of evaluating tunnel diameter at various depths, depth of the liquefaction sand lens, changes in the angle of friction inside the sand lens as well as changes in tunnel lining thickness at the sand lens location.

2-Modeling Method

The present study aims to model a loose sand lens inside a hard clay sediment during liquefaction. FLAC 3D is used to create the three-dimensional model of the sand lens and also to determine the changes in both pore water pressure and the effective stress due to liquefaction within the sand lens. For this purpose, the various forces exerted on the tunnel lining will be calculated under a dynamic load along with the resulting deformations inside a clay deposit that lacks any sand lenses. Then, the same process will be repeated with the inclusion of a sand lens. The effect of the sand lens on the forces exerted on the tunnel lining along with the relationship between the location of the sand lens and ground surface settlement will be analyzed under different seismic loads.

3-Creating Reference Models

3.1. Model A

Figure 2 shows a tunnel with a diameter of 6.9 meters and a depth of 10 meters, which is dug in three dimensions inside clay. The bedrock is set to 50m below the tunnel and the model is extended by 5D from either side of the tunnel in order to minimize the influence of lateral borders on the results. This will reduce the error rate caused by stress to around 5% enabling us to disregard the border influence on the analysis. The width of the model was chosen as 20 meters according to the figure. This width was chosen because it was possible to model a sand lens inside it in subsequent modeling. For dynamic analysis, the model is meshed as per Figure 2. FLAC 3D uses rectangular meshes for its problem solving.

The dimension of the mesh must be small enough as to allow the diffusion of the shear waves simulated in the model. According to studies by Lismer and Colmayer, wavelength is the determining factor for proper wave diffusion in numerical models. The chosen wavelength depends on the dimensions of the elements placed along the diffusion path which must be between 1/8th to 1/10th of the wavelength itself. Any dynamic force with a frequency above 25Hz will be filtered out [15]. Since liquefaction conditions require the soil to be fully saturated, the underground water level will be set as equal to the ground level.

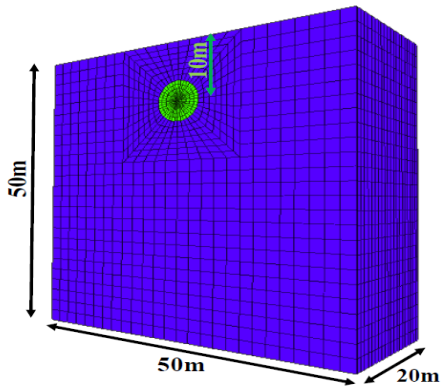

Fig.2. Model A and its mesh structure.

3.1. Model B

According to Figure 3, the dimensions of the reference model B are similar to the reference model A, with the difference that in the reference model B, a sand lens inside the clay was modeled. The dimensions of the sand lens with the width and height of 16 meters, length of 10 meters and depth of 10 meters are as shown. A tunnel with the mentioned specifications is dug through the sand lens. This loose sand lens will undergo local liquefaction under dynamic load and its effect on the tunnel lining and ground surface settlement shall be determined under various different conditions.

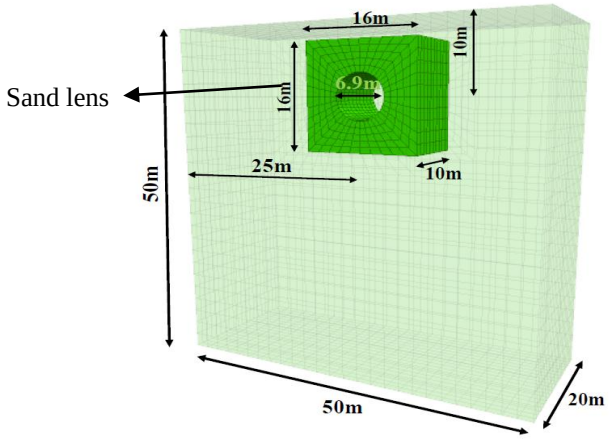

Fig. 3. Model B and the location of the sand lens.

4-Soil Properties

Table 1 shows the soil properties of the clay deposit used in model A, along with the characteristics of the sand lens used in model B. These are based on the literature review[16-18] and the parameters used in the VELACS project[19] (soil parameters found in Nevada, US).
Since the objective is to analyze the liquefaction effect in the sand lens, the FLAC modeling must be made as to reflect changes in volume, pore water pressure and effective stress during liquefaction while under dynamic load. The Finn behavioral model will be used for this purpose. This model was introduced by Martin et al. in 1975 and shows the relationship between volumetric strain increment ($\Delta\varepsilon_{vd}$) and cyclic shearing strain (γ) as per the following equation [18]:

$$\Delta\varepsilon_{vd} = C_1(\gamma - C_2\varepsilon_{vd}) + \frac{C_3\varepsilon_{vd}^2}{\gamma + C_4\varepsilon_{vd}}$$

C_1 through C_4 are coefficients which are obtained from cyclical triaxial experiments. These coefficients were set to 0.76, 0.52, 0.2 and 0.5 respectively, based on the study by Pashangpishe[20].

5-Loading Method and Loading Conditions

An important factor that affects the behavior of the soil environment is dynamic loading. This loading is introduced as the dynamic force in the analysis depending on its type, size, duration and frequency characteristics. There are various methods by which a dynamic force can be introduced to the model in FLAC 3D, two of which will be used in the present study.
In the first method, since the most common type of load exerted during an earthquake is a shear wave emanating from the bedrock towards the surface, a harmonic acceleration is defined as per the following, and exerted from the bottom of the model:

$$\ddot{u_g} = A_g \sin(2\pi f t)$$

In the above equation, Ag, f and t represent the amplitude, frequency and duration of the dynamic loading respectively. In accordance with Khoshnoudian[15], the loading amplitude and acceleration frequency used in the reference model was set to 0.1g and 1Hz respectively, along with a loading duration of 10 seconds. This duration will allow the simulation process to arrive at a consistent state and thus demonstrate the effect of the dynamic load more clearly. Damping is selected locally in the reference model and is equal to 5%. The free conditions set for the borders of the model allow them to act as an absorber and prevent any waves from reflecting back into the model during the simulation process.

In the second method, acceleration time history is used for seven different earthquakes according to Table 2 with different frequency content and response spectra of incoming earthquakes is used with scaled maximum acceleration according to Figure 4. Damping and free field conditions for dynamic boundaries was considered as 5%. In this condition, the reflection of waves in the model is prevented and the boundaries act as absorbing boundaries. All the acceleration maps were scaled to the maximum acceleration of 0.3 g in the analysis. The acceleration of the selected maps based on the characteristics of the case study, such as the land type, the condition of the bedrock, and the distance from the fault, were extracted from the nearby area (less than 10 km) from the PEER site (24) and used in the analysis after applying corrections.

Table. 1
Soil properties of the clay deposit and the sand lens.

Soil Parameters	Behavioral Model	Shear Modulus (MPa)	Bulk Modulus (MPa)	φ (^{0})	C (kpa)	γ_d (kN/m^3)	K (m/s)
Model A	Mohr-Coulomb	25	50	30	40	17	10^{-6}
Model B	Finn	20	30	25	0	15	10^{-4}

Table. 2
Characteristics of the input waves for various earthquakes.

Earthquake	Imperial Valley	Loma Prieta	Northridge	Chi-Chi	Duzce	Montenegro	El Mayor
Station	El Centro Array	Capitola	Mulho	Chylol	Lamont	Ulcinj	Cerro Prieto Geothermal
RSN(s)	6	752	953	1244	1615	4458	5825

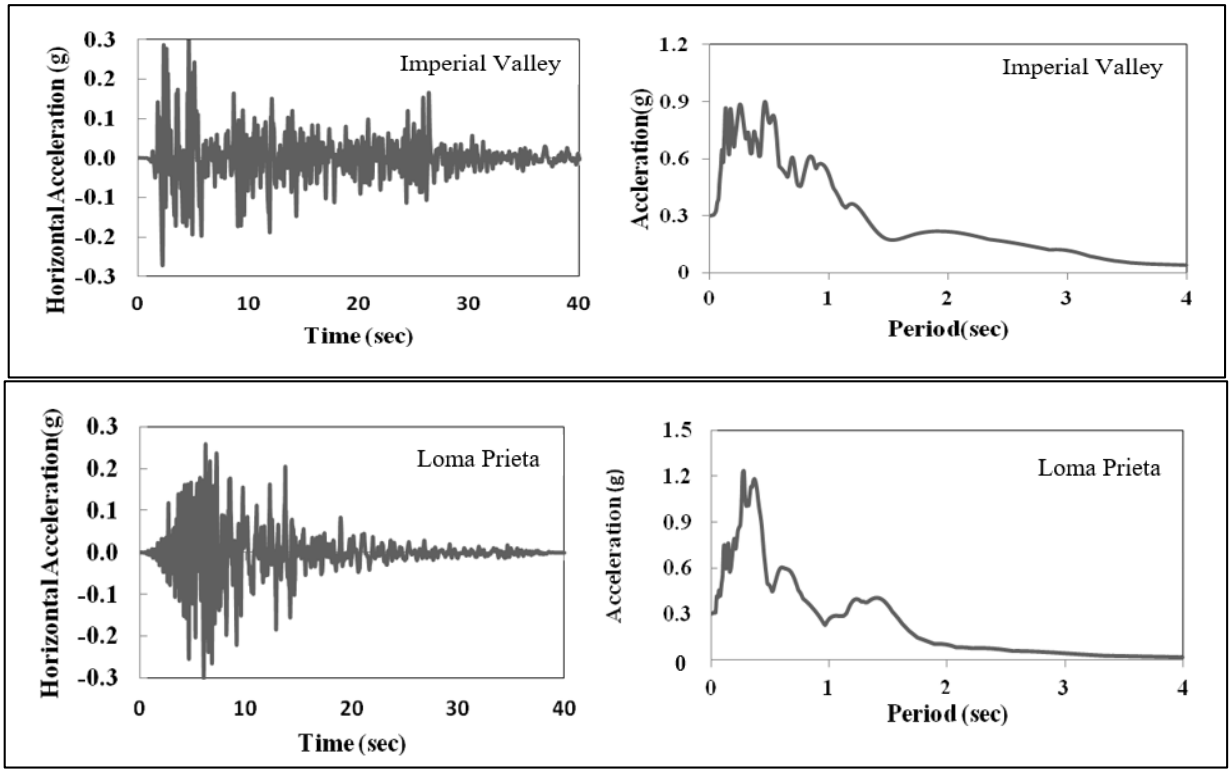

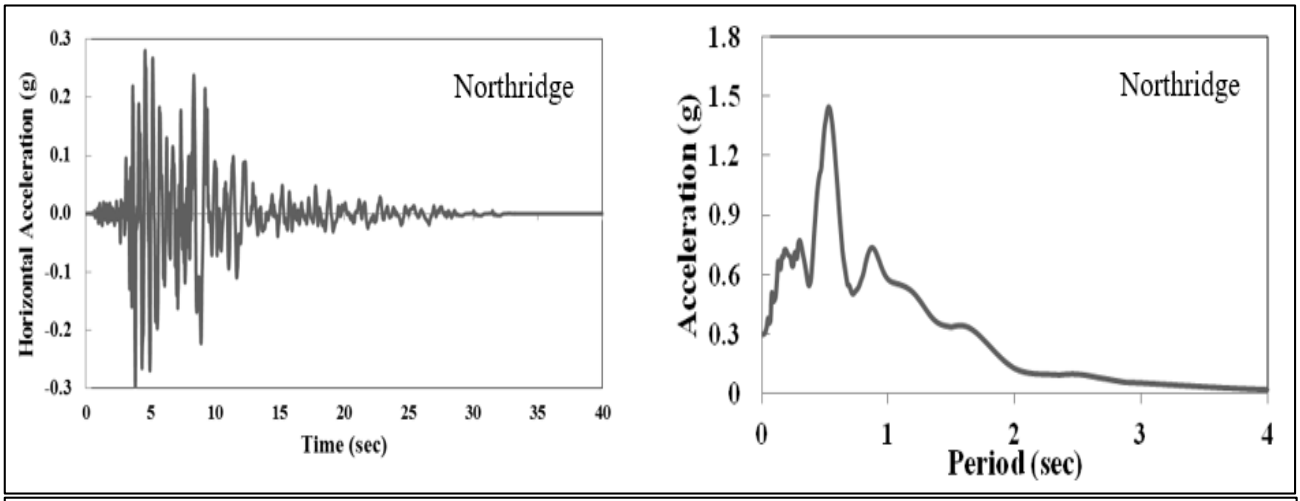
Northridge
Horizontal Acceleration (g)
Time (sec)
Northridge
Acceleration (g)
Period (sec)

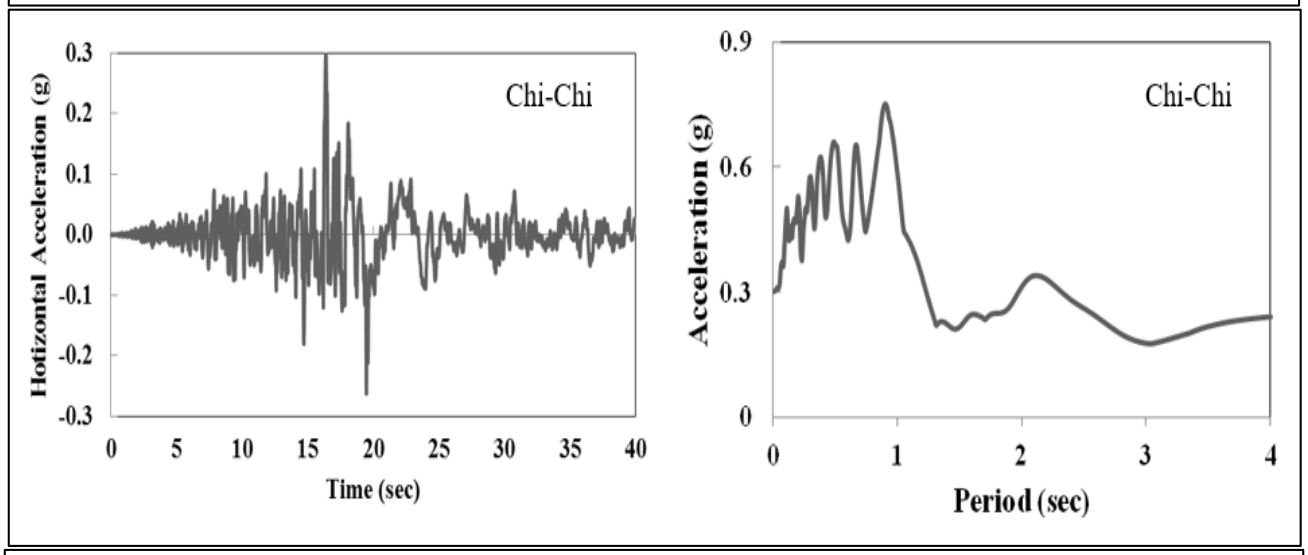
Chi-Chi
Hotizontal Acceleration (g)
Time (sec)
Chi-Chi
Acceleration (g)
Period (sec)

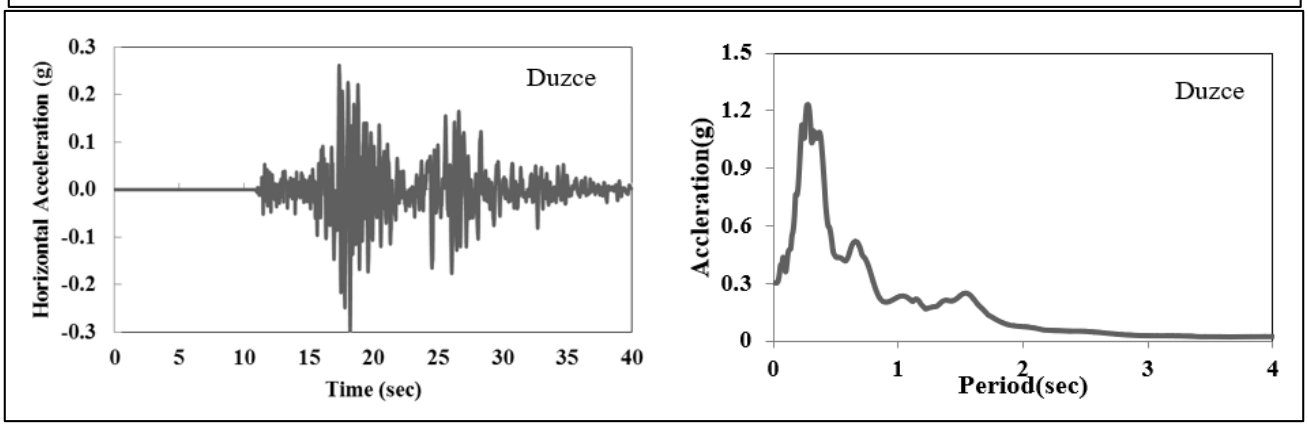
Duzce
Horizontal Acceleration (g)
Time (sec)
Duzce
Accleration(g)
Period(sec)

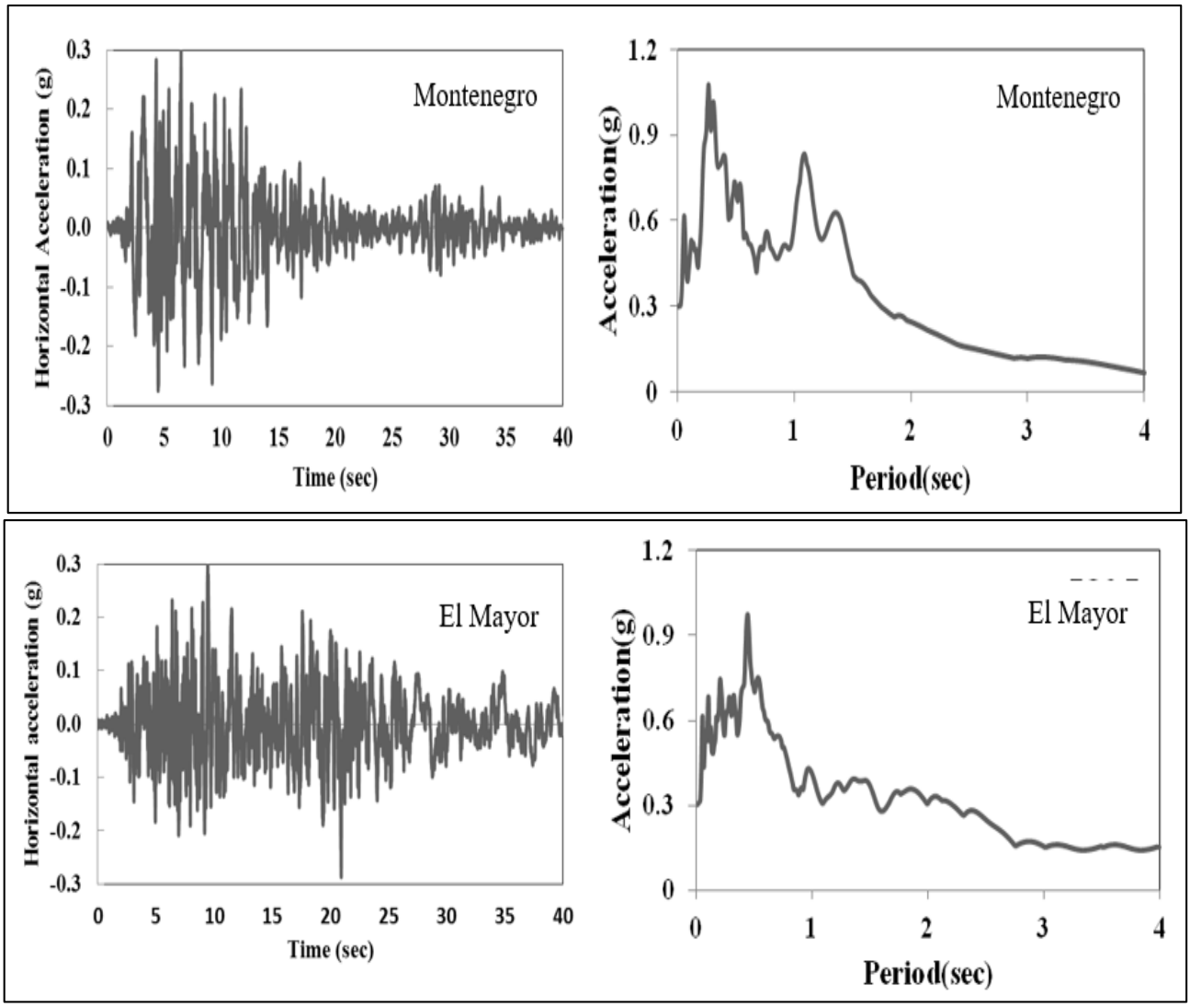

Fig.4. Earthquake Response spectrum and the Acceleration time history obtained from the records including a maximum acceleration of 0. 3g and a damping of 5

6-Tunnel Lining Properties

6.1. Meshing and how to Model the Tunnel

The meshing and modeling of the tunnel used in FLAC 3D can be seen in Figure 5. The location of the tunnel is such that it passes through the flowing sand lens. This is a tunnel with an outer diameter of 6.9m with a tunnel lining which is 30cm thick at a depth of 10 meters from the ground. A comparative case study would be the underground tunnel located in the city of Esfahan, Iran. The elasticity modulus was equal to $E=2.236\times10^7$ kN/m^2.

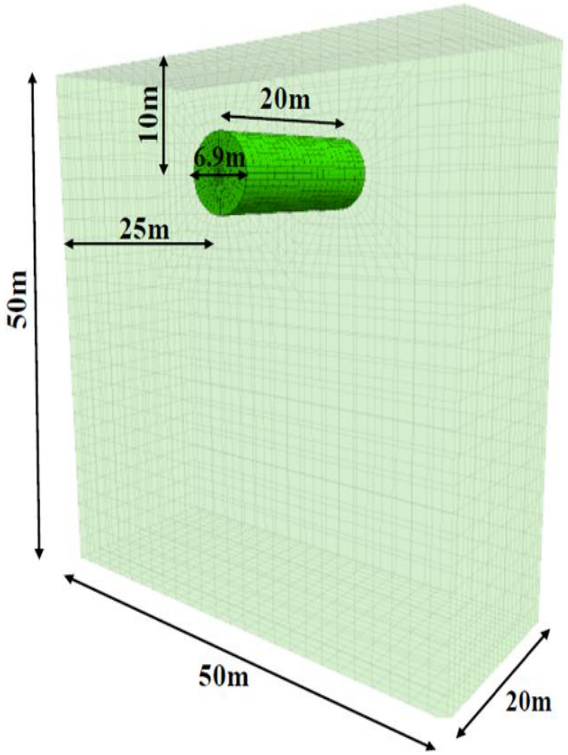

Fig. 5. Tunnel modeling and its position

7.Reference Model Analysis

7-1. Model A

The 6.9 diameter tunnel is situated 10m below the surface inside a clay depot and is being subjected to the dynamic load specified in the first method above. As was mentioned before, the underground water level is set equal to the surface level. The results of the analysis indicate that the longer the duration of the dynamic load, the higher the maximum axial force and bending moment exerted on the tunnel lining will be. The pore water pressure also rises but not to the extent as to cause reduced effective stress leading to soil liquefaction.

Graph 1 shows the pore water pressure at different depths inside the clay by applying dynamic force, which shows the constant pore water pressure under the tunnel at depths of 14 and 15 meters. The dynamic force caused 16mm of ground surface settlement above the tunnel axis and a maximum bending moment in the tunnel lining equal to 16.7(ton-m). These results are in agreement with those obtained by both Mair et al. [21] and Mir M. Hosseini et al. [5] in their respective studies which was done on cohesion soils.

7-2. Model B.

Liquefaction of a sand lens in close proximity of the tunnel can affect pore water pressure and effective stress which can in turn lead to the exertion of new forces and new deformities in the soil and tunnel. In reference model B, the dynamic load described in the second method was used. Comparing the two together reveals that the pore water pressure has increased in model B due to liquefaction in the sand lens. Graph 2 indicates the increase in pore water pressure inside the sand lens after applying the earthquake load at depths of 14 and 15 meters. The pore water pressure at the depths of 14 and 15 meters per second is zero and before the earthquake load is equal to 135 and 150 kilopascals. After applying the load of the Imperial Valley earthquake for 40 seconds, the total pore water pressure in the sand lens at the depth of 14 and 15 meters increased and reached 205 and 220 kilopascals. Also, the excess pressure of pore water was close to 70 kilopascals. This increase in pore water pressure reduced the effective stress and thus lead to liquefaction of the sand lens.

Based on the analysis performed, as the stresses and deformities in the soil increase, the forces present in the tunnel lining are reduced. This may be due to soil displacement caused by liquefaction of the sand lens. Table 3 shows the maximum axial force and bending moment exerted on the tunnel lining along with the amount of ground surface settlement obtained from various earthquakes. The differences in the values are due to changes in horizontal acceleration and frequency content present in each earthquake record. Figure 6 indicates the land surface settlement above the sand lens under the Imperial Valley earthquake. This settlement was due to liquefaction in the sand lens and was obtained as 89 mm. Figure 7 indicates the value of the maximum axial force on the tunnel lining in the part of the sand lens subjected to the Imperial Valley earthquake. Liquefaction in the sand lens caused this value to reach 43.9 tons in the sand lens part.

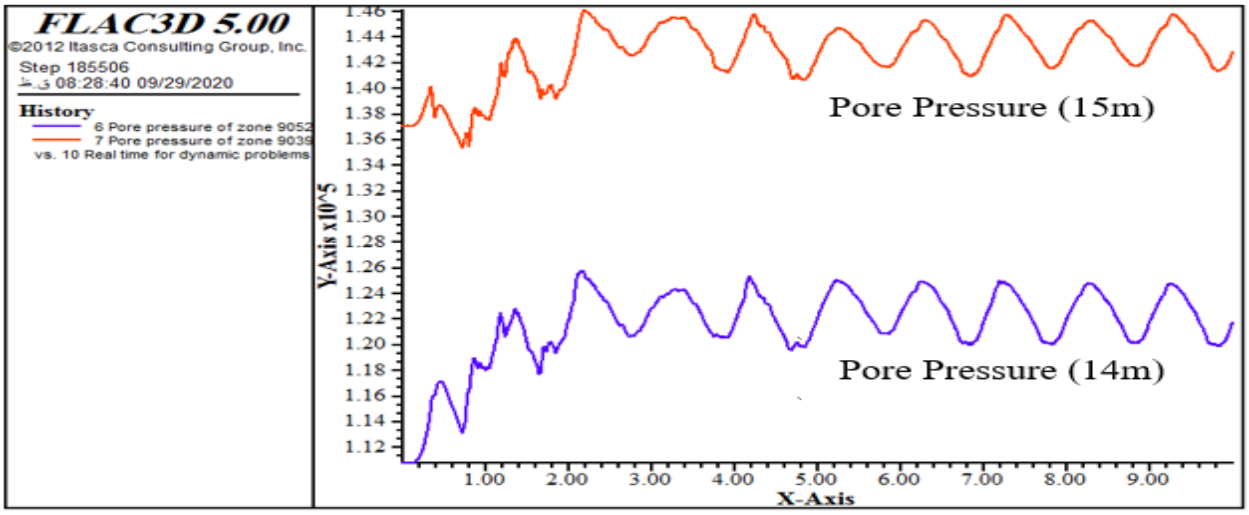

Graph. 1 The Pore water pressure of reference model A.

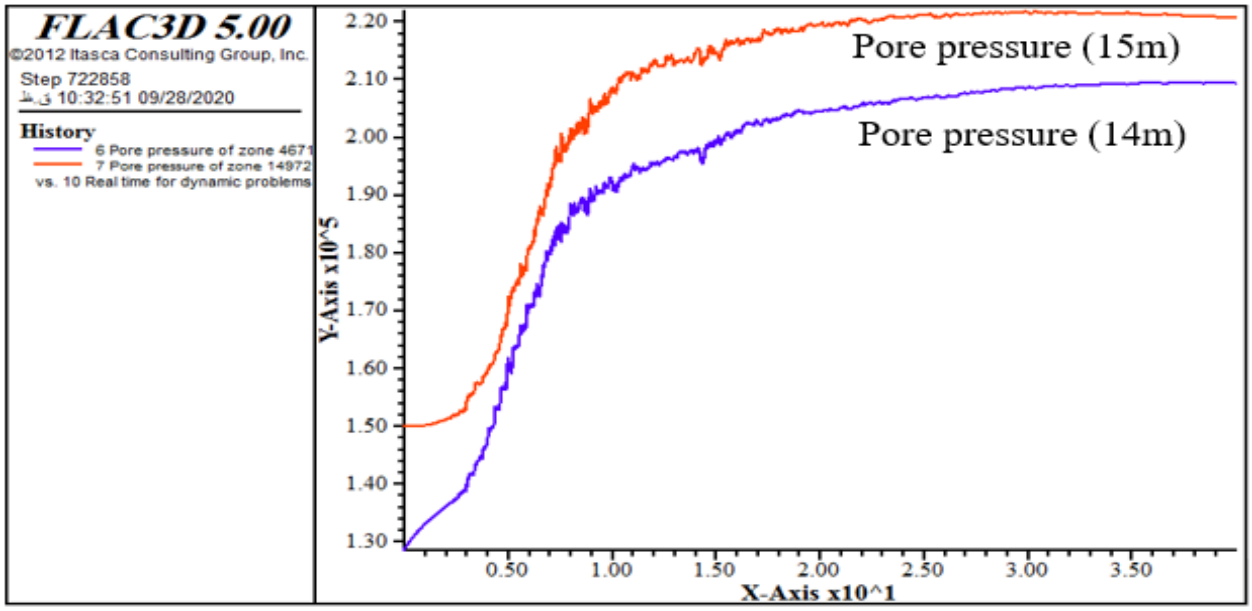

Graph. 2 Increased pore water pressure in the sand lens from the Imperial Valley earthquake.

Table. 3
Axial force, bending moment and ground surface settlement due to liquefaction in each earthquake.

Earthquake	Imperial Valley	Loma Prieta	Northridge	Chi-Chi	Duzce	Montenegro	El Mayor
Axial Force (ton)	43.9	39.57	48.03	41.09	35.14	55.51	43.79
Bending Moment (ton-m)	8.17	5.74	8.24	8.65	7.31	8.82	6.8

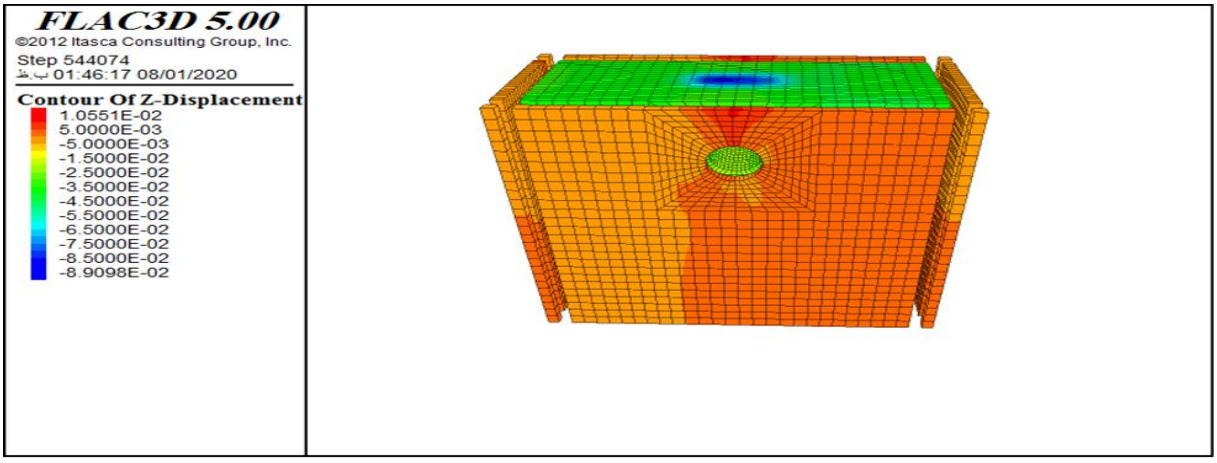

Fig. 6 Ground surface settlement due to liquefaction.

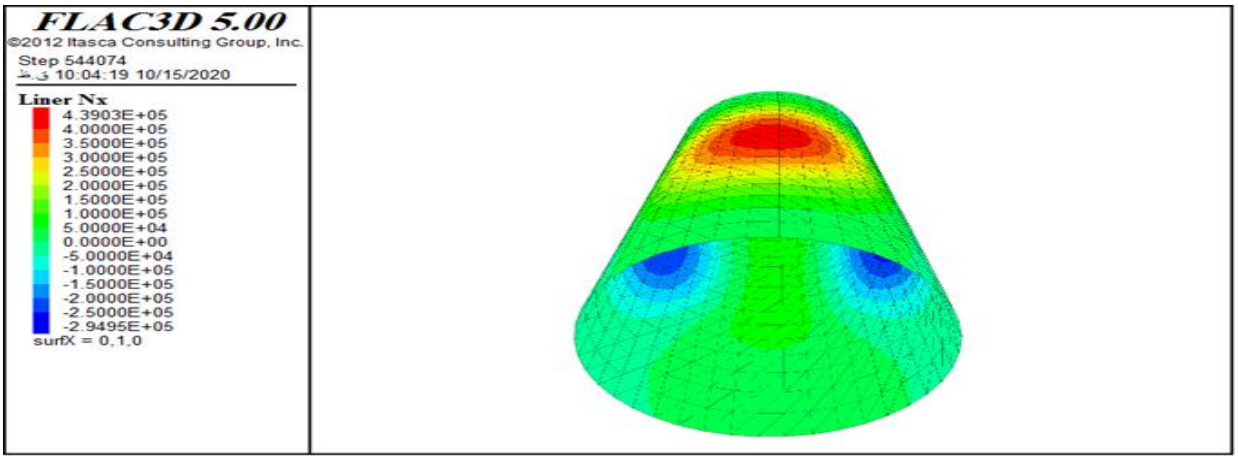

Fig.7 Axial force exerted on the tunnel lining due to the liquefaction effect of the sand

8-Tunnel Diameter Inside the Sand Lens

Increased tunnel diameter inside the sand lens reduces the amount of ground surface settlement. When tunnels with a larger diameter are built in a sand lens, the amount of soil susceptible to liquefaction around the tunnel is reduced which also lowers the amount of ground surface settlement. Graph 3 shows the amount of ground surface settlement from each earthquake based on the tunnel diameter. It is apparent that increasing tunnel diameter from 6.9m to 10m or 12m will lead to a reduction of ground surface settlement by an average of 30% and 50% respectively, compared to reference model B.

Increasing the tunnel diameter means a larger volume of the sand lens soil is removed from the tunnel surroundings which reduces the effects of liquefaction on the tunnel. By reducing the liquefaction effect, tunnel displacement is also reduced which results in increased axial force and bending moment exerted on the tunnel lining. Graph 4 shows the maximum bending moment exerted on the tunnel lining at the location of the sand lens based on the tunnel diameter. It is apparent that increasing tunnel diameter from 6.9m to 10m or 12m will increase the bending moment exerted on the tunnel lining by an average of 26% or 76% respectively, compared to reference model B.

Graph 5 shows axial forces exerted on the tunnel lining at the location of the sand lens based on the tunnel diameter. It is apparent that increasing tunnel diameter from 6.9m to 10m or 12m will increase the axial force exerted on the tunnel lining by an average of 8% or 21% respectively, compared to reference model B. It must be noted that the trends of certain graphs are related to changes in the horizontal acceleration and frequency content

Of each earthquake record.

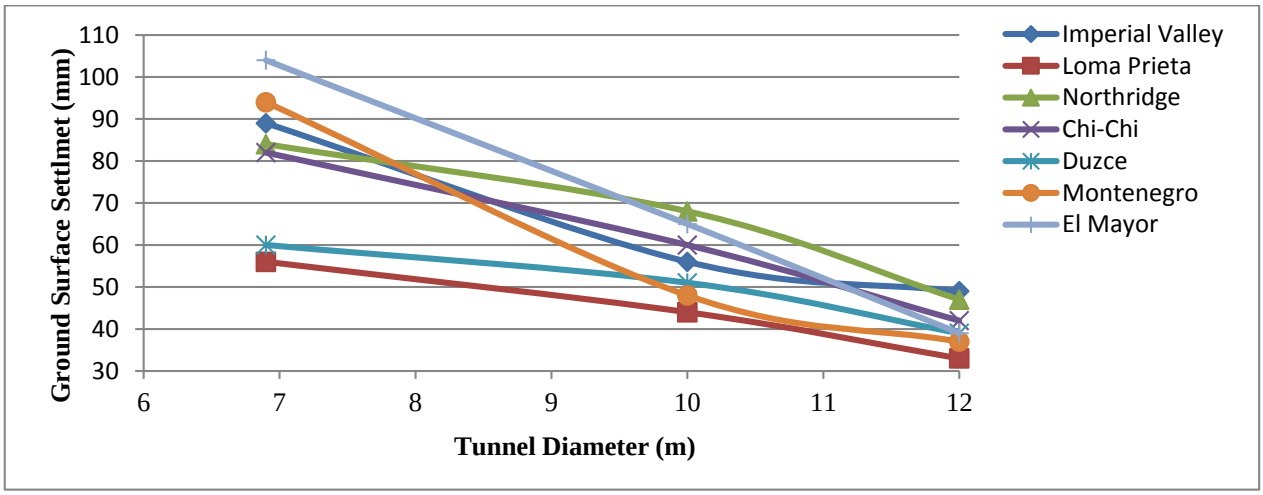

Graph 3. Ground surface settlement in relation to tunnel diameter.

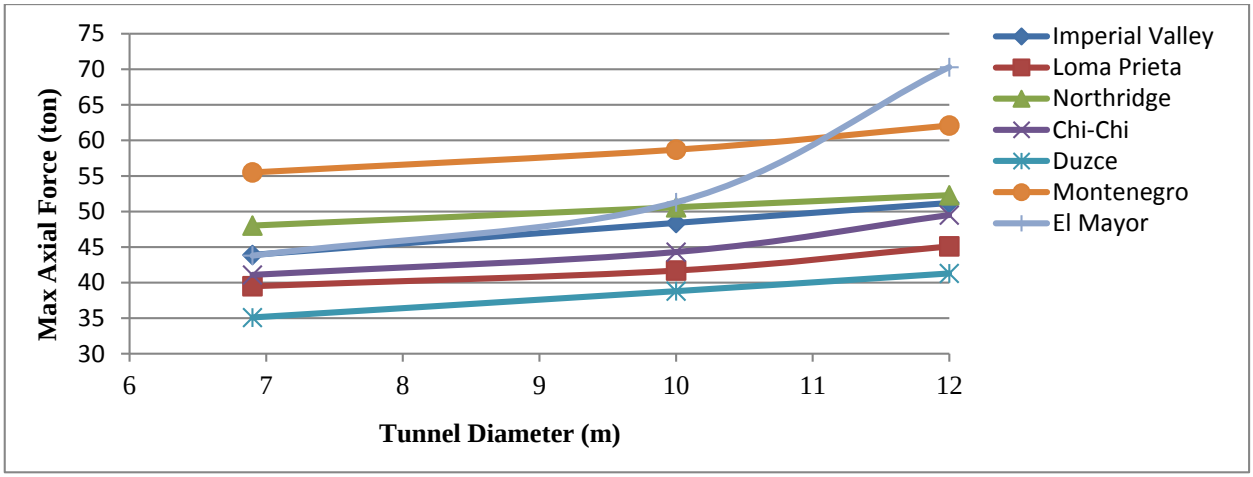

Graph 4. Bending moment exerted on the tunnel lining in relation to tunnel diameter.

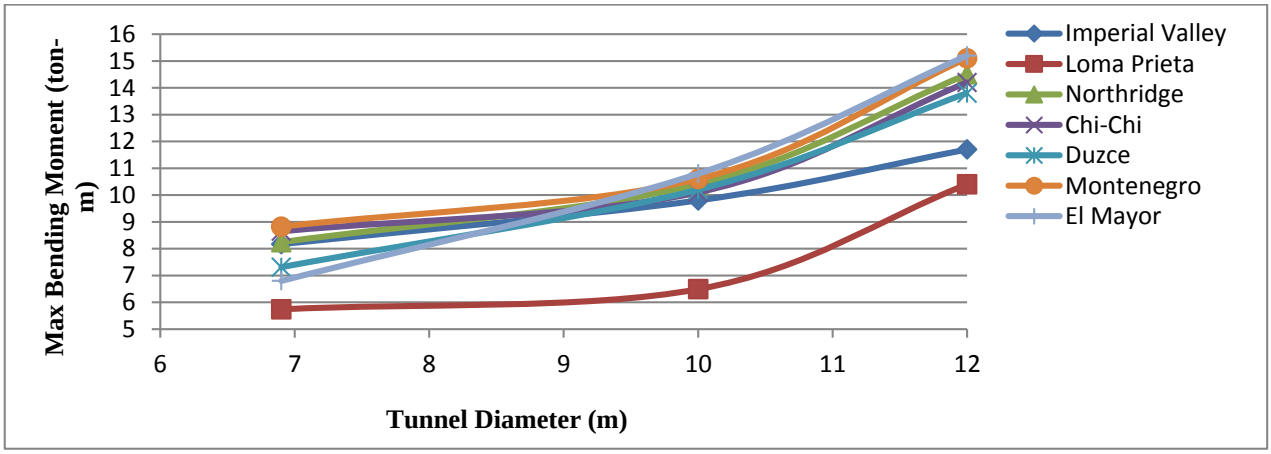

Graph 5. Maximum axial force exerted on the tunnel lining in relation to tunnel diameter.

9-Angle of Friction Inside the Sand Lens

Changing the sand lens angle of friction in reference model B allows us to analyses the amount of ground surface settlement and the forces exerted on the tunnel lining in each of the earthquakes. As is apparent from graph 6, changing the soil angle of friction from 25° to 20° will increase ground surface settlement by an average of 6% compared to reference model B. However, going from 25° to 30° will decrease ground settlement by 6%. This is because increased soil angle of friction creates a denser material resulting in reduced liquefaction effects.Graphs 7 and 8 show the maximum bending moment and maximum axial force exerted on the tunnel lining at the location of the sand lens based on soil angle of friction. It is apparent that changing the soil angle of friction from 25° to 20° will reduce maximum bending moment by an average of 4% and maximum axial force by an average of 1% compared to reference model B. However, going from 25° to 30° will increase maximum bending moment by an average of 5% and maximum axial force by an average of 1.5%. This is due to the reduced lateral earth pressure compared to the vertical earth pressure exerted by the soil above the tunnel crown which can cause larger moments and forces in the tunnel lining at the location of the sand lens.

Graph 6. Ground surface Settlement in relation to soil angle of friction.

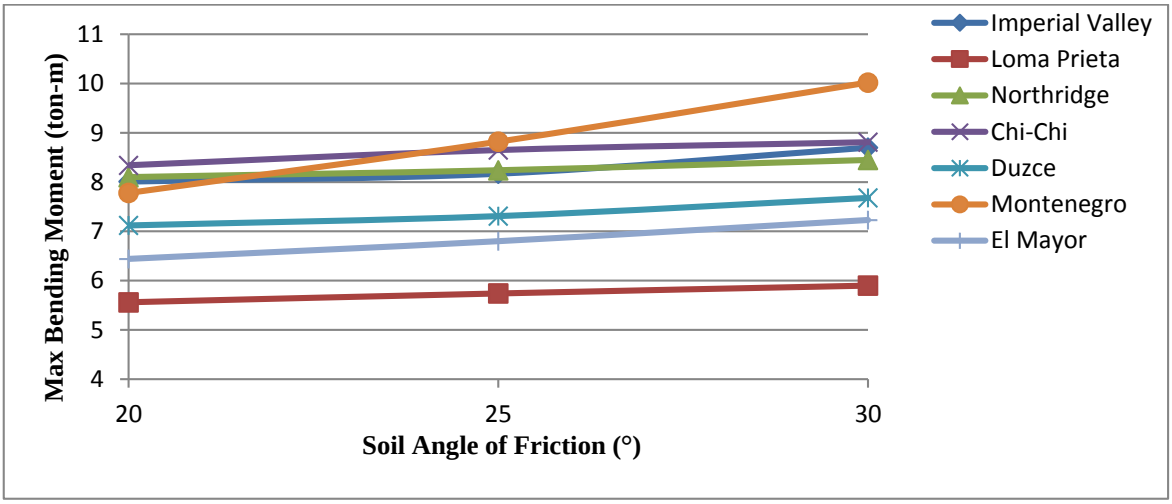

Graph 7. Maximum bending moment exerted on the tunnel lining in relation to soil angle of friction.

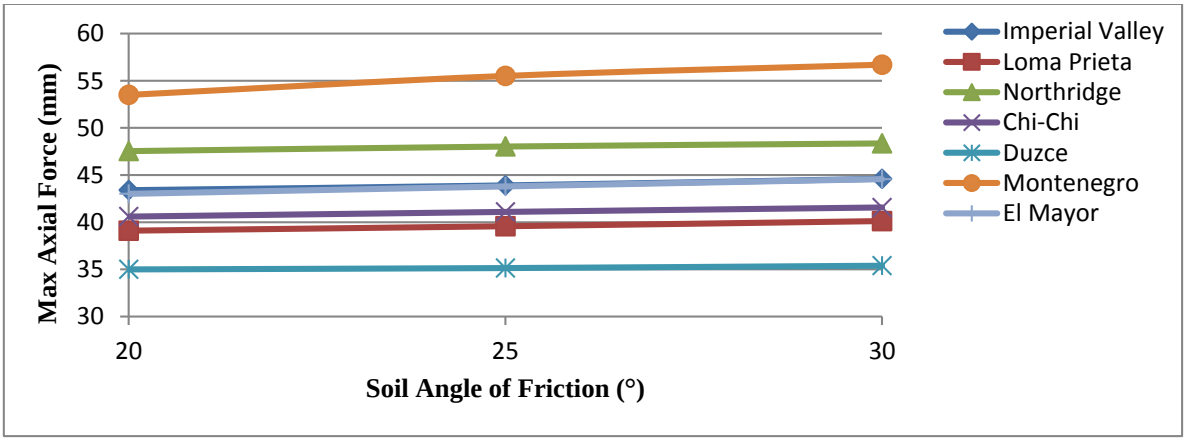

Graph 8. Maximum axial force exerted on the tunnel lining in relation to soil angle of friction.

10-Tunnel Lining Thickness at the Sand Lens Location

Changing the tunnel lining thickness at the location of the sand lens and subjecting the tunnel to the various earthquakes enables us to analyze ground surface settlement and the forces exerted on the tunnel lining. As is apparent from graph 9, changing the tunnel lining thickness from 30cm to 20cm will result in a 2.4% increase in ground surface settlement compared to reference model B. However, going from 30cm to 40cm will reduce ground surface settlement by 3.5%. It seems that tunnel lining thickness does not significantly affect ground surface settlement after liquefaction of the sand lens. Graph 10 shows the maximum bending moment exerted on the tunnel lining based on the tunnel lining thickness. A tunnel lining thickness of 20cm reduces maximum bending moment by 18% while a tunnel lining thickness of 40cm increases it by 26% compared to reference model B. At lower thickness, the tunnel lining is lighter and less stable in response to liquefaction which means it cannot bear the axial force and bending moment exerted onto it. Higher lining thickness at the sand lens location reduces lining deformation due to its higher weight and thus the tunnel lining can bear a higher axial force and bending moment.Graph 11 shows the maximum axial force exerted on the tunnel lining at the location of the sand lens based on tunnel lining thickness. It is apparent that a tunnel thickness of 20cm reduces the maximum axial force exerted on the tunnel lining by an average of 4% compared with reference model B. At a thickness of 40cm however, the maximum axial force exerted is increa sed by an average of 3%.

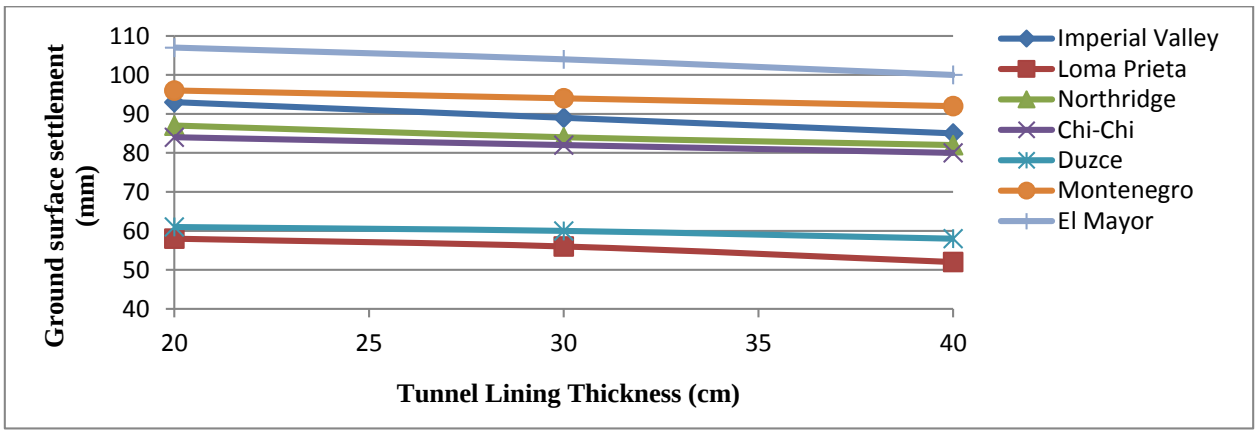

Graph 9 .Ground surface settlement in relation to tunnel lining thickness at lens location.

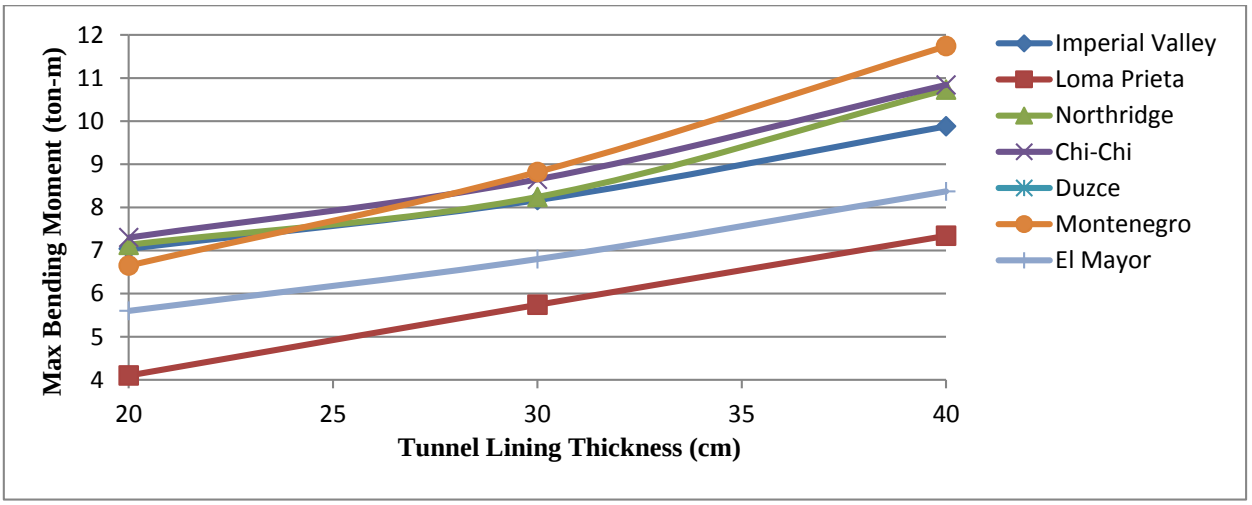

Graph10. Maximum bending moment exerted on tunnel lining in relation to lining thickness at the lens location.

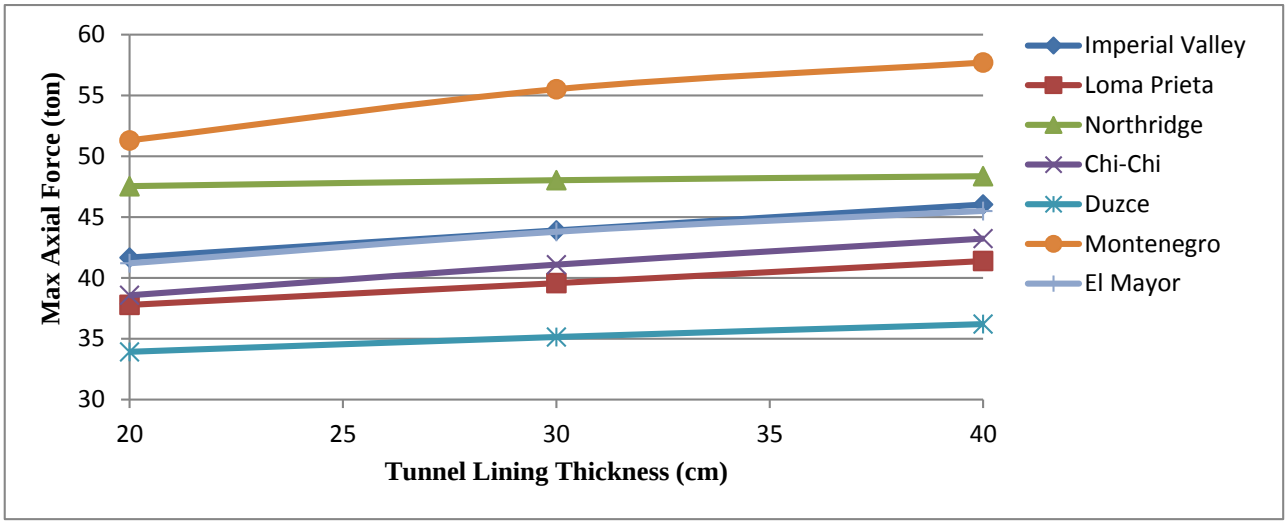

Graph 11. Maximum axial force exerted on the tunnel lining in relation to lining thickness at the lens location.

11-Depth of the Sand Lens and its Effect on the Liquefaction of Surrounding Soil

Changing the depth of the sand lens in which the tunnel is built can affect the amount of ground surface settlement. The results indicate that increasing the depth of the sand lens reduces the amount of ground surface settlement. This is due to the reduced liquefaction effect of the sand lens as its depth is increased and vice versa. As is apparent from Graph 12, a 2-meter depth increase corresponds to an average reduction in ground surface settlement of 30.8% while a 2-meter depth reduction corresponds to an average increase in ground surface settlement of 36% compared to reference model B.

Figure 8 indicates the amount of land surface settlement above the sand lens under the Imperial Valley earthquake when the center of the sand lens and the tunnel depth is 12 meters. According to the figure, the value of ground level settlement was obtained as 3.58 mm, which is according to the explanation mentioned in the above section.

Figure 9 indicates the maximum axial force on the tunnel lining in the part of the sand lens under the Imperial Valley earthquake when the center of the sand lens and the depth of the tunnel are 2 meters higher than reference model B (12 meters deep). Due to the liquefaction of the sand lens, this value was obtained equal to 54.3 tons, which shows that with the increase in the depth of the sand lens, the axial force on the tunnel increases.

Graphs 13 and 14 show the maximum bending moment and axial force exerted on the tunnel lining based on the sand lens depth. As is apparent, a 2m increase in the depth of the sand lens corresponds to a 35.7% and 14.4% average increase in the maximum bending moment and axial force exerted on the tunnel lining respectively. This is due to the increase in soil overburden pressure on the tunnel crown. Reducing the sand lens depth however, corresponds to a 28% reduction in the maximum bending moment and a 10.8% reduction in the axial force exerted on the tunnel lining respectively.

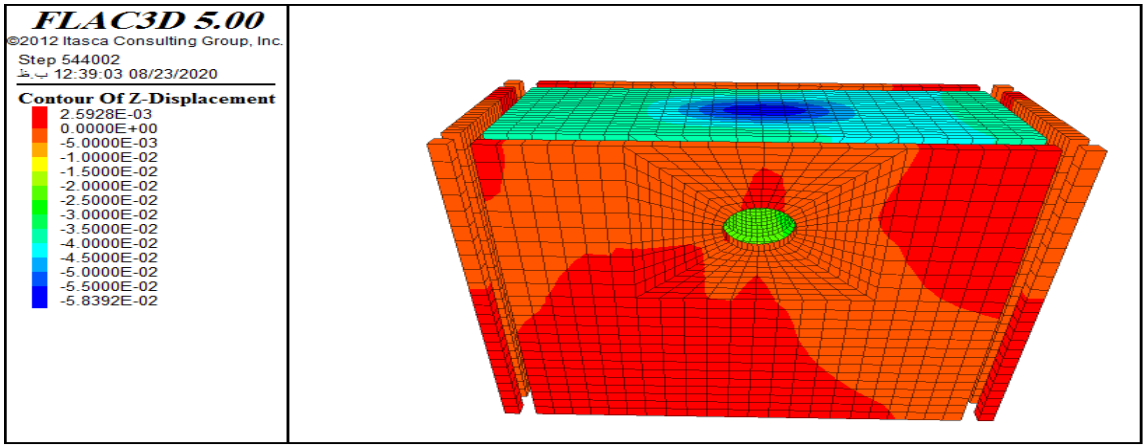

Fig 8. Amount of ground surface settlement due to the liquefaction effect of the sand lens.

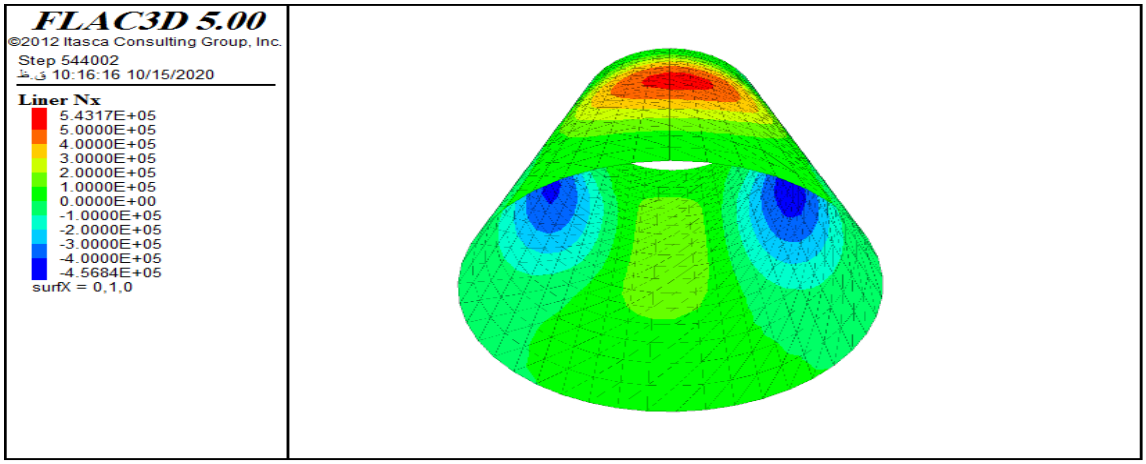

Fig 9. Axial force exerted on the tunnel lining due to the liquefaction effect of the sand lens.

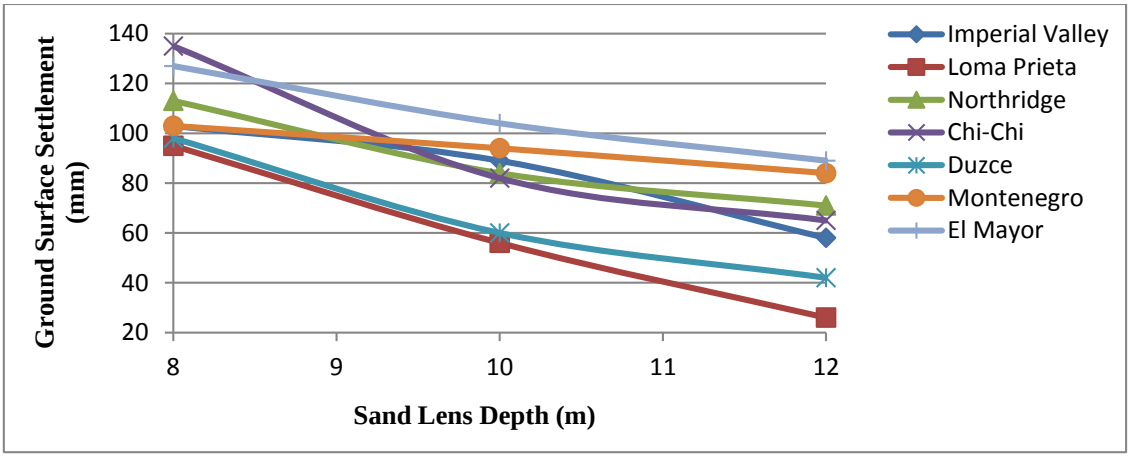

Graph12. Ground surface settlement in relation to sand lens depth.

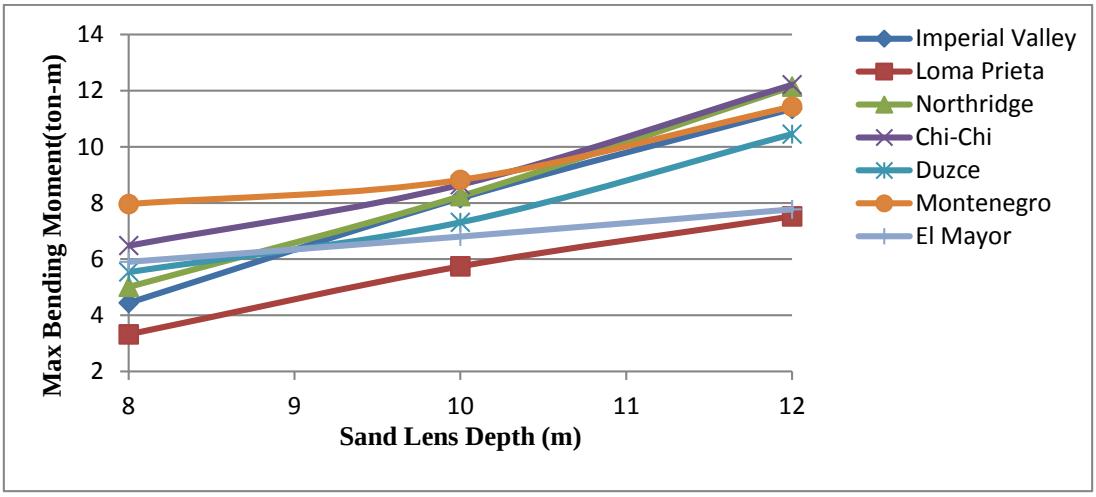

Graph 13. Maximum bending moment exerted on the tunnel lining in relation to sand lens depth.

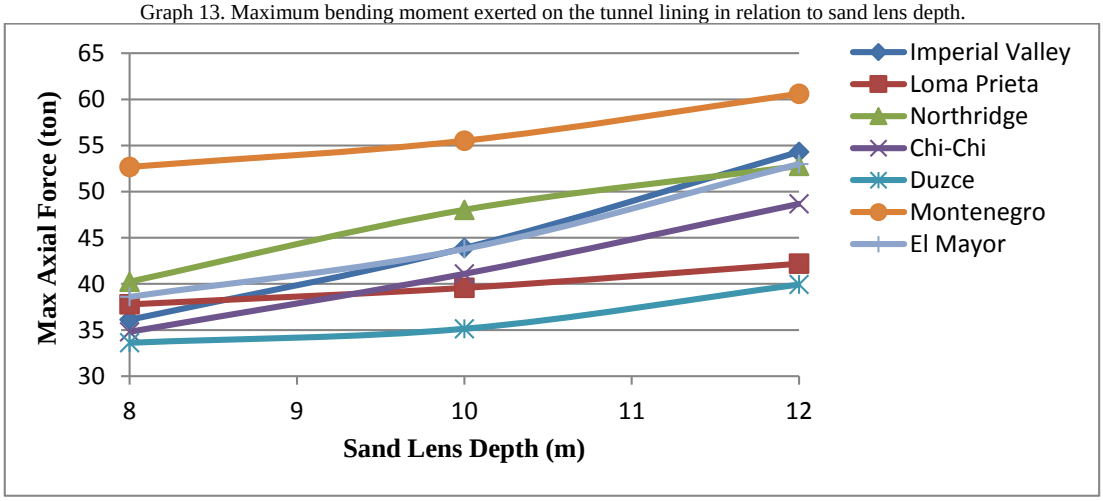

Graph 14. Maximum axial force exerted on the tunnel lining in relation to sand lens depth

.

12-Tunnel Lining Thickness at the Sand Lens Location

Changes in tunnel diameter at different depths within the liquefaction sand lens has major effects on ground surface settlement. Results reveal that increasing tunnel diameter at different depths within the sand lense reduces the amount of liquefiable soil and thus reduces the effects of liquefaction. Ground surface settlement is therefore
reduced while the maximum bending moment and axial force exerted on the tunnel lining at the location of the sand lense is increased. Graph 15 shows the relation between changes in tunnel diameter inside the sand lense and the amount of ground surface settlement at different depths during the exertion of the Imperial Valley earthquake and compares it to reference model B. It is apparent that changing tunnel diameter inside the sand lense at depths lower than that of reference model 2 has a considerable effect on ground surface settlement which must be taken into account in the design. Conversely, at depths above that of reference model 2, changes in tunnel diameter have very little effect on ground surface settlement.
Graph 16 and 17 shows the relation between changes in tunnel depth inside the liquefaction sand lens and maximum bending moment and axial force exerted on the tunnel lining for different tunnel diameters while exerting the Imperial Valley earthquake and compares it to reference model 2. Based on the analysis performed on these figures, it can be concluded that changes in tunnel diameter inside the sand lens at depths above that of
reference model B has very little effect on the bending moment and axial force exerted on the tunnel lining. Conversely, changes in tunnel diameter at depths lower

than that of reference model 2 has a significant effect on the bending moment and axial force exerted on the tunnel lining at the location of the liquefaction sand lens which must be taken into account when designing and constructing these types of tunnels.The study of Azadi et al. [6] was conducted in 2018 with the aim of Effect of Width Variation of Liquefiable Sand Lens on Surface Settlement Due to Shallow Tunneling. This study investigated land surface subsidence and changes in sand lens width. The sand lens was modeled with three different widths compared to its initial position. Then it evaluated the effect of liquefaction of the sand lens on the deformations and anchors created in the tunnel lining and stated that increasing the width of the sand lens from 10 to 15 meters does not have much effect on the bending anchor, but after this width, the effect of the bending anchor on the tunnel lining is highly noticeable. In addition, the study indicated that increasing the width of the sand lens leads to an increase in land surface settlement. So that, if the width of the sand lens is increased from 10 to 20 meters, the subsidence of the land surface will increase about 3 times. The study above, only investigated the width of the sand lens, but this article, the depth of the sand lens was examined. In addition, it has studied the changes in the depth and diameter of the tunnel inside the sand lens and the change in the thickness of the tunnel lining and the separate effect of each of them on the settlement of the ground and the axial force and bending anchor on the tunnel lining is obtained.

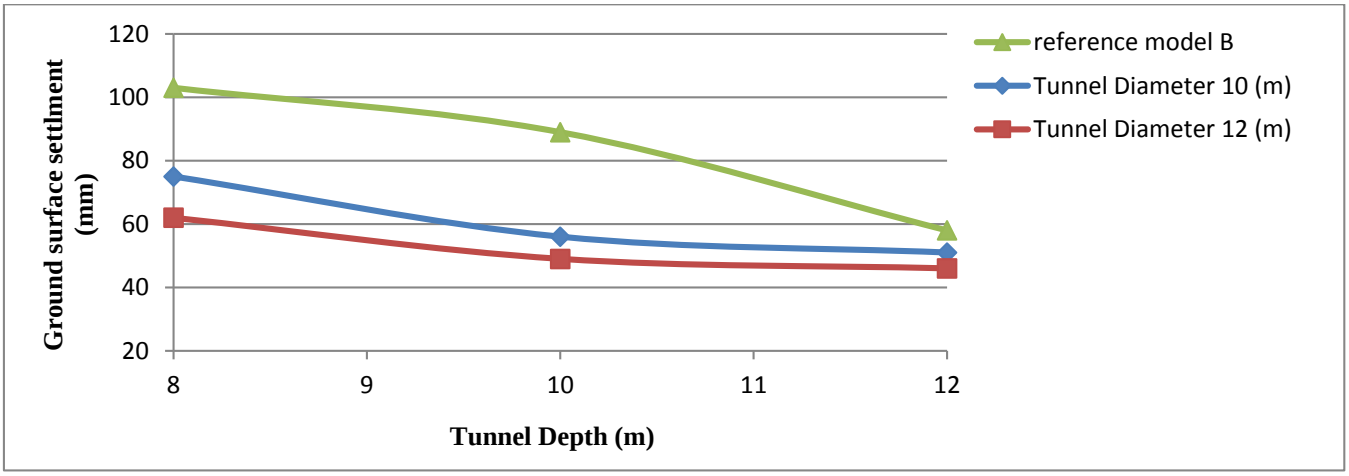

Graph 15. Changes in tunnel depth within the liquefaction sand lens compared to ground surface settlement for different tunnel diameters.

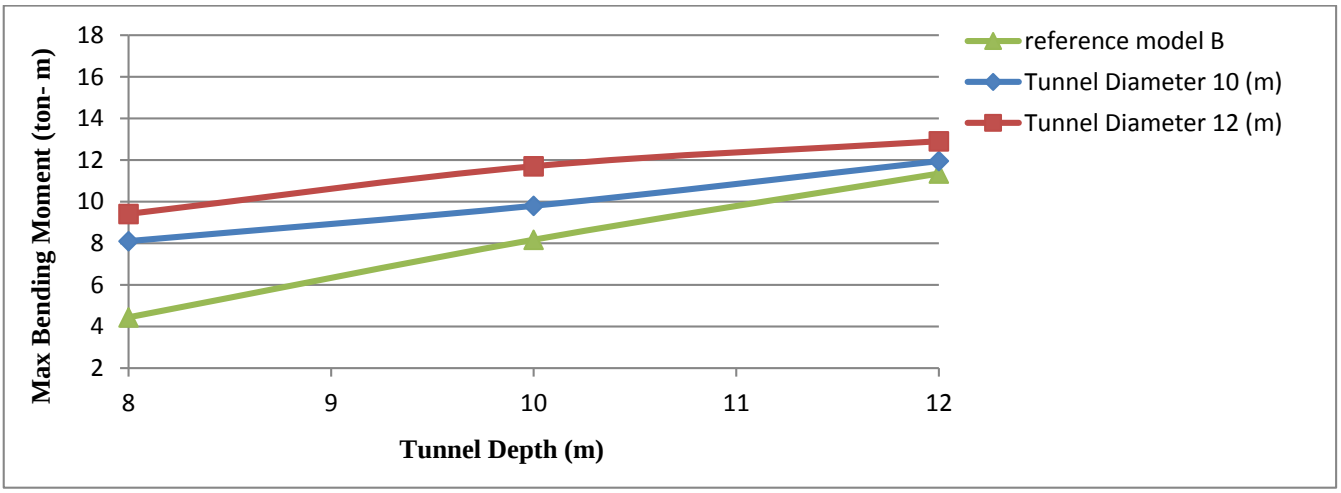

Graph 16. Changes in tunnel depth compared to the maximum bending moment exerted on the tunnel lining at the liquefaction sand lens location for different tunnel depths.

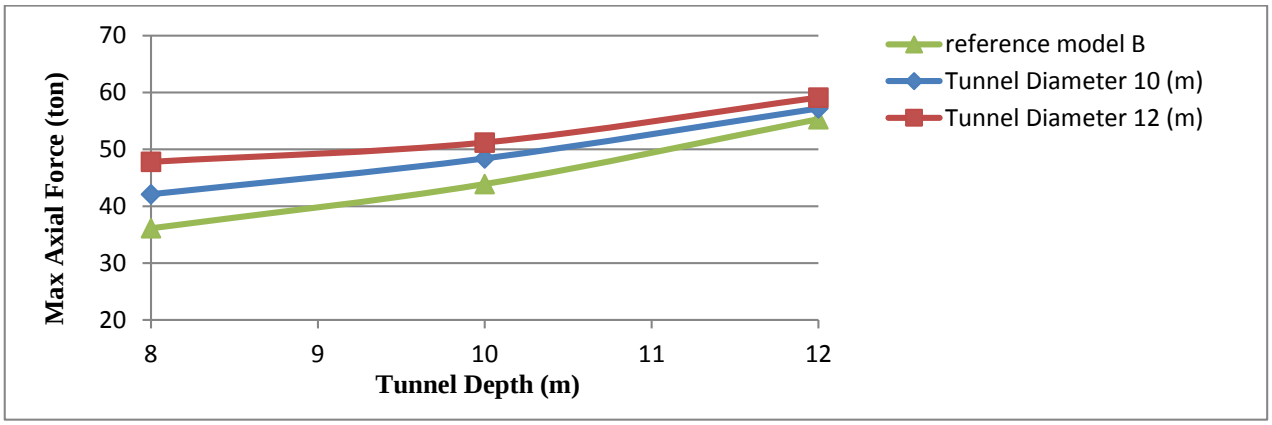

Graph 17. Changes in tunnel depth compared to the maximum axial force exerted on the tunnel lining at the liquefaction sand lens location for different tunnel depths.

13-Conclusion

The present study was aimed at analyzing sand lens liquefaction effects on the tunnel lining. Based on the data obtained and the analysis performed, the conclusion of the present study can be summarized as follows:

1. Increasing the friction angle of the sand lens from 25° to 30° in (reference model B) will reduce ground settlement by 6%. This is because a higher angle of friction creates a denser material which is less susceptible to the liquefaction effects of the sand lens. Reducing the soil friction angle from 25° to 20° will increase ground surface settlement by 6%.
2. Changing the soil angle of friction at the location of the sand lens from 25° to 30° will increase the bending moment and the maximum axial force exerted on the tunnel lining by 5% and 1.5% respectively. This is due to the reduced lateral earth pressure compared to the perpendicular earth pressure of the top soil above the tunnel crown which creates larger moments on the tunnel lining.
3. Increasing tunnel diameter from 6.9m (reference model B) to 10m or 12m will reduce ground surface settlement at the sand lens area by 30% or 50% respectively. This is because a larger amount of soil susceptible to liquefaction is excavated when building larger tunnels which results in less ground settlement. The maximum axial force exerted on the tunnel lining will increase by 8% at a diameter of 10m and 21% at a diameter of 12m. Maximum banding moment exerted on tunnel lining will also increase by 26% at a diameter of 10m and 76% at a diameter of 12m. This is because with less susceptible soil around the tunnel, the liquefaction effect of the sand lens is reduced leading to less tunnel displacement which in turn means that a larger axial force and bending moment is exerted.
4. Changing the tunnel diameter from 30cm (reference model B) to 20cm or 40cm will increase ground surface settlement by 2.4% or decrease it by 3.5% respectively. It seems that tunnel diameter has no significant effect on ground surface settlement after sand lens liquefaction. Maximum axial force exerted on the tunnel lining will decrease by 4% at a diameter of 20cm and increase by 3% at a diameter of 40cm. Maximum bending moment exerted on the tunnel lining at the sand lens area will decrease by 18% at a diameter of 20cm and
increase by 26% at a diameter of 40cm. This is because decreasing the thickness of the tunnel lining will reduce the tunnel weight and lower its stability against liquefaction at the sand lens area. Increasing the thickness will limit lining deformation due to increased weight and so the tunnel can bear a larger axial force and bending moment at the sand lens area during liquefaction.
5. Reducing the depth of the sand lens from 10m (reference model B) to 8 meters will increase ground settlement by 36% while increasing the depth to 12m will reduce ground surface settlement by 30.8%. This means that lower a sand lens depth results in a greater liquefaction effect and more ground surface settlement. A 2m increase in sand lens depth results in a 35.7% increase in the maximum bending moment and a 14.4% increase in maximum axial force exerted on the tunnel lining. This is due to the increase in soil overburden

pressure on the tunnel crown. A 2m decrease in sand lens depth results in a 28% reduction in the maximum bending moment and a 10.8% reduction in the maximum axial force exerted on the tunnel lining.

6. In regards to tunnels built at depths below 10 meters (reference model B), changes in tunnel diameter has a considerable effect on ground surface settlement, maximum bending moment and axial force exerted on the tunnel lining within the sand lens, which must be taken into account when building such tunnels. As for tunnels built at depths higher than that of reference model B, changes in tunnel diameter has very little effect on ground surface settlement, maximum bending moment and axial force.

It can thus be concluded that the location and properties of the sand lens along with changes in tunnel diameter and lining thickness can directly affect the forces exerted on the tunnel lining and the amount of ground surface settlement from liquefaction. The findings of the present study can be very useful in the decision-making process where tunnels are to be excavated in liquefaction susceptible sand lenses embedded in clay deposits.

Acknowledgement

The authors gratefully acknowledge the assistance provided by the University of California PEER Strong Motion Database.

Reference

[1] M. Azadi, "Efect of Soil Liquefaction on Shield Tunnels," M.Sc. Thesis Submitted in Civil Eng, Faculty of Amirkabir University of Technology, Iran, p. 242, 2007.

[2] L. E. Vallejo, "The liquefaction of sand lenses during an earthquake," in Earthquake Engineering and Soil Dynamics II—Recent Advances in Ground-Motion Evaluation, 1988: ASCE, pp. 493-507.

[3] Shukri, "Investigation of liquefaction potential of sand lenses," Phd. Thesis Submitted in Civil Eng, Faculty of Amirkabir University of Technology, Iran., 1996.

[4] K. S. Beheshti, "Study of the behavior of saturated sand lenses in soil layers under dynamic loading," M.Sc. Thesis Submitted in Civil Eng, Faculty of Amirkabir University of Technology, Iran., 1998.

[5] M. Azadi and L. S. Bryson, "Effect of Width Variation of Liquefiable Sand Lens on Surface Settlement Due to Shallow Tunneling," in International Congress and Exhibition" Sustainable Civil Infrastructures: Innovative Infrastructure Geotechnology", 2018: Springer, pp. 155-163.

[6] Unified Facilities Criteria (UFC)-DoD. Design of Buildings to Resist Progressive Collapse, Department of Defense; 2005.

[7] B. J. T. Unutmaz and u. s. technology, "3D liquefaction assessment of soils surrounding circular tunnels," vol. 40, pp. 85-94, 2014.

[8] Y. Zhang, J. Yang, and F. J. E. F. A. Yang, "Field investigation and numerical analysis of landslide induced by tunneling," vol. 47, pp. 25-33, 2015.

[9] Z. Haiyang et al., "Seismic responses of a subway station and tunnel in a slightly inclined liquefiable ground through shaking table test," vol. 116, pp. 371-385, 2019.

[10] G. Zheng, W. Zhang, W. Zhang, H. Zhou, and P. J. U. S. Yang, "Neural network and support vector machine models for the prediction of the liquefaction-induced uplift displacement of tunnels," 2021.

[11] Q. Liao, Q.-Q. Fan, and J.-J. Li, "Translation control of an immersed tunnel element using a multi-objective differential evolution algorithm," Computers & Industrial Engineering, vol. 130, pp. 158-165, 2019.

[12] S. Nokande, A. Haddad, and Y. Jafarian, "Shaking Table Test on Mitigation of Liquefaction-Induced Tunnel Uplift by Helical Pile," International Journal of Geomechanics, vol. 23, no. 1, p. 04022243, 2023.

[13] S. C. Chian, K. Tokimatsu, S. P. G. J. J. o. G. Madabhushi, and G. Engineering, "Soil liquefaction–induced uplift of underground structures: physical and numerical modeling," vol. 140, no. 10, p. 04014057, 2014.

[14] M. Azadi, S. M. M. J. T. Hosseini, and U. S. Technology, "The uplifting behavior of shallow tunnels within the liquefiable soils under cyclic loadings," vol. 25, no. 2, pp. 158-167, 2010.

[15] J. Lysmer and R. L. J. J. o. t. e. m. d. Kuhlemeyer, "Finite dynamic model for infinite media," vol. 95, no. 4, pp. 859-878, 1969.

[16] F. Khoshnoudian, I. J. S. Shahrour, and foundations, "Numerical analysis of the seismic behavior of tunnels constructed in liquefiable soils," vol. 42, no. 6, pp. 1-8, 2002.

[17] H. Liu, E. J. C. Song, and Geotechnics, "Seismic response of large underground structures in liquefiable soils subjected to horizontal and vertical earthquake excitations," vol. 32, no. 4, pp.

223-244, 2005.

[18] M. Azadi, S. M. M. J. T. Hosseini, and u. s. technology, "Analyses of the effect of seismic behavior of shallow tunnels in liquefiable grounds," vol. 25, no. 5, pp. 543-552, 2010.

[19] R. Popescu, J. H. J. S. D. Prevost, and E. Engineering, "Comparison between VELACS numerical 'class A'predictions and centrifuge experimental soil test results," vol. 14, no. 2, pp. 79-92, 1995.

[20] Y. Pashangpishe, "Mechanism of soil deformation due to double lenses liquefaction and critical depth determination," M. Sc. Thesis Submitted in Civil Eng., Faculty of Amirkabir University of …, 2004.

[21] R. Mair, R. Taylor, and A. J. G. Bracegirdle, "Subsurface settlement profiles above tunnels in clays," vol. 43, no. 2, pp. 315-320, 1993.